Arabian Journal of Chemical and Environmental Research

Vol. 11 Issue 1 (2024) 16–43

Adsorptive removal of methylene blue dye from synthetic wastewater using acid and base activated *Parkia biglobosa* seed pod

Z. Hashim[1], M. B. Ibrahim[2], B. Usman[3], A. S. Usman[4], A. A. Muhammad[5]

[1]*Department of Pure and Industrial Chemistry, Bayero University, P.M.B.3011, BUK, Kano-Nigeria*
Email: zaharahasheem61@gmail.com
[2]*Department of Pure and Industrial Chemistry, Bayero University, P.M.B.3011, BUK, Kano-Nigeria*
Email: mbibrahim.chm@buk.edu.ng
[3]*Department of Pure and Industrial Chemistry, Bayero University, P.M.B.3011, BUK, Kano-Nigeria.*
[4]*Department of Chemistry, Faculty of Science, Yobe State University, Dmaturu, Nigeria.*
[5]*Department of Pure and Industrial Chemistry, Bayero University, P.M.B.3011, BUK, Kano-Nigeria.*

Received 01 May 2024, Revised 26 July 2024, Accepted 26 July 2024

Cited as: *Z. Hashim, M. B. Ibrahim, B. Usman, A. S. Usman, A. A. Muhammad, Adsorptive removal of methylene blue dye from synthetic wastewater using acid and base activated Parkia biglobosa seed pod, Arab. J. Chem. Environ. Res. 11(1) (2024) 16-43*

Abstract

The adsorption capacity of activated carbon derived from *Parkia biglobosa* (PB) seed pod has been studied using the batch adsorption method. The adsorbents were characterized using Fourier transform infrared (FTIR) spectroscopy and scanning electron microscopy (SEM). C-H, O-H, C≡N, and C=C groups were observed upon PB, HPB (H_3PO_4-activated *Parkia biglobosa)* and KPB (KOH-activated *Parkia biglobosa*), which showed slight alteration after activation and subsequent adsorption processes. The pH of point zero charge (pH_{pzc}), moisture, and ash content of the absorbents were investigated. The pH_{pzc} of PB, HPB, and KPB were determined to be 6.6, 6.8, 7.2 respectively. Optimization of agitation time, initial concentration, adsorbent dosage, temperature, and pH. The highest adsorption capacity of the dye was found to be 91.48, 71.70 and 75.52 mg/g onto PB, HPB and KPB respectively. The kinetic studies reveal that adsorption follows a pseudo-second-order model with R^2 values close to unity, and q_{exp} 19.26 is nearly equal to q_{cal} 19.27 onto PB adsorbent. Adsorption isotherm studies showed the best fit with the Langmuir model with values 0.9969 and 0.9945 onto PB and KPB and then HPB with value 0.9838, correlates best with Freundlich isotherm model. Investigation of the thermodynamic parameters (negative ΔG and ΔH) showed that all the adsorption processes are spontaneous and exothermic. The results obtained suggest that the adsorbents are potential candidates for use in the remediation of industrial wastewater.

Keywords: *Adsorption, Activated charcoal, Methylene blue, Adsorption kinetics, Thermodynamic*

*Corresponding author.
E-mail address: zaharahasheem61@gmail.com

ISSN : 2458-6544

1. Introduction

Water resources have been contaminated, and the environment has been harmed by industrial growth, particularly in the textile sector (Charumathi and Das, 2012; Dargo *et al*., 2014; Le *et al*., 2016). The textile industry is the largest consumer of dye, releasing approximately 10,000 tons per year (Yagub *et al*., 2014; Shaban *et al*., 2017). Cancer and other negative health impacts are brought on by non-adsorbed dyes in wastewater (Mojsov *et al*., 2016). Additionally, dyes are harmful to aquatic life because they lower dissolved oxygen and abstract photochemical and biological processes (Rafatullah *et al*., 2010; Üner *et al*., 2017). Protection of the environment depends on wastewater remediation through the elimination of dyes.

Methylene blue, (MB) is a thiazine dye that is basic in nature, broad uses for methylene blue (MB) include coating paper stock, temporary hair color, colouring cottons and wools, and dyeing paper (Haque *et al*., 2011). Methylene blue can have certain negative consequences even if it is not particularly dangerous. Increased heart rate, vomiting, shock, the formation of Heinz bodies, cyanosis, jaundice, quadriplegia, and tissue necrosis are among symptoms of acute exposure to methylene blue in people (Hameed & Ahmad, 2009; Khalid *et al*., 2012; Aaddouz et al., 2023).

Adsorption (Schouten et al., 2007), electrochemical treatment, biological treatment, membrane filtration, coagulation, photochemical degradation and oxidation (Akartasse *et al*., 2022; Zsilák *et al*., 2014; Errami *et al*., 2012 & 2013; Bouri *et al*., 2012) are just a few techniques used to remove colours from wastewater (Yagub *et al*., 2014; Aly *et al*., 2019). Various methods have been attempted to remove color from wastewater, but none have been entirely successful due to their limitations. Biological treatment processes are toxic, coagulation decolorizes insoluble dyes, and photochemical degradation slows down due to synthetic dyes' light stability. Economic removal remains a major issue (Singh *et al*., 2018). Adsorption emerged as the most advantageous approach among them due to its low operational cost, low sensitivity to pollutants, high efficiency, economic feasibility, and simplicity of design (Rafatullah *et al*., 2010; Khalid *et al*., 2012; Lamhmdi *et al*., 2014)

Adsorption is a surface phenomenon that involves the adhesion of gases, liquids, and solids to the surface of the adsorbent (Yunusa & Ibrahim, 2020). It is a reliable and effective approach to handling industrial and domestic effluents (Dabrowski, 2001). An adsorbate is a substance that sticks to or concentrates at the surface, whereas an adsorbent is a substance on which adsorption is taking place (Dabrowski, 2001; Mokif, 2019; Yunusa & Ibrahim, 2020). Adsorption is primarily caused by the physisorption and chemisorption processes, physical sorption is the result of van der Waals forces of attraction, while chemisorption depends on the creation of a strong chemical bond between the adsorbent and the adsorbate (Yagub *et al*., 2014;).

Other materials used as adsorbents, including activated carbon (which is a well-known adsorbent offered because of its high adsorption capacity, large surface area, and microporous structure), are more expensive, less accessible, and less renewable than agricultural waste (Aly *et al*., 2019). Low-cost adsorbents have two main benefits: wastewater remediation and waste management, making them a demanding field (Rafatullah *et al*., 2010).

Activated carbon is the most widely used sorbent material of all those proposed for removing pollutants from wastewater (Akter *et al*., 2021). Adsorption of activated carbons is an excellent replacement for more expensive treatment technologies since it is highly effective at eliminating a variety of colours from wastewater. However, there are a number of disadvantages to activated carbon, such as the cost, regeneration problems, non-selectivity, and ineffectiveness against disperse and vat dyes (Khalid *et al*., 2012). The use of carbon based on somewhat expensive starting materials is thus not justified for the bulk of pollution control applications. Many employees have been compelled to look for the less expensive options (Yagub *et al*., 2014)**.**

An agricultural waste material, such as raw maize cob, exhausted coffee ground powder (Namane *et al*., 2003), saw-dust (Garg *et al*., 2003), seed pods, black cumin, neem leaf, pineapple leaf, and pine tree leaves, have been used by many researchers in dye remediation of contaminated wastewater. Agricultural wastes are less expensive, more readily available, and more renewable than other materials utilized as adsorbents. (Dutta *et al*., 2021)

African locust bean (Parkia biglobosa) tree belongs to the family Fabaceae. It belongs to the genus Parkia which belongs to the tribe Parkieae. Parkia biglobosa is found in so many African countries. In Nigeria, it is found everywhere. Traditionally, it is used as food and medicine, therefore, it's of high commercial value in the West African region. The plant is reported to contain carbohydrates, proteins, vitamins, tannins and flavonoids, and it's known to have antimalarial, anthelminthic, antibacterial, antivenom, antidiabetic, antioxidant and antihypertensive properties (Biglobosa, 2014). In this work, we report the results of the adsorption of a cationic dye Methylene blue (MB), over a PB, HPB and KPB adsorbents.

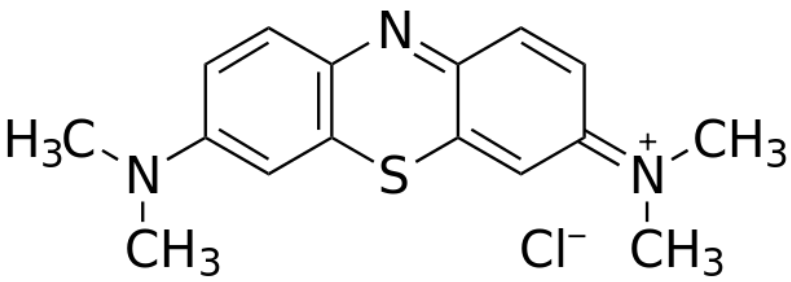

Figure 1.1. Methylene Blue

1. Experimental work

2.1. materials and methods

2.1.1 Adsorbate

The stock solution of methylene blue dye (1000 mg/L) was prepared, by dissolving 1g of the dye in 100 cm^3 beaker and then transferred to 1000 cm^3 volumetric flask and made-up to the mark with distilled water. The desired experimental concentration (10-100 mg/L) was prepared by appropriate dilution of the stock solution with distilled water.

2.2. preparation of adsorbent

Parkia biglobosa seed pod was sourced from Kurmi local market in Kano State, Nigeria. The pod was washed thoroughly with water and then with distilled water to remove dirt and dust and other impurities. The sample was sun dried for about 48 hours, and then redried in an oven to constant weight at 105^oC temperature. The dried pod was then grounded using mortar and pestle, sieved using 0.2µm sieve, to obtain fine powder of the biosorbent. The sieved fine power of biosorbent was then divided into three portions. The first portion was stored in an air-tied container and leveled as PB adsorbent, without any further treatment. The second portion of the sample was impregnated with 85% concentrated H_3PO_4 in the ratio (2:1) wt./wt (Pam and Abdullah, 2022) and the third portion with KOH plus 100 cm^3 distilled water in the same ratio, followed by manual mixing for about 30min and was then dried separately at 110 ^oC in an electric oven for 24hours. Using muffle furnace, the samples was carbonized at 600 ^oC temperature (Pam and Abdullah, 2022). The samples was cooled, leached with 0.1 M H_3PO_4 and 0.1 M KOH as appropriate then washed thoroughly with distilled water until a neutral (pH≈6.9) was attained (Yunusa and Ibrahim, 2020). The desired activated carbon was obtained after drying in an oven at 110 ^oC for 24 hours.

2.3. preparation of adsorbent

Parkia biglobosa seed pod was sourced from Kurmi local market in Kano State, Nigeria. The pod was washed thoroughly with water and then with distilled water to remove dirt and dust and other impurities. The sample was sun dried for about 48 hours, and then redried in an oven to constant weight at 105^oC temperature. The dried pod was then grounded using mortar and pestle, sieved using 0.2µm sieve, to obtain fine powder of the biosorbent. The sieved fine power of biosorbent was then divided into three portions. The first portion was stored in an air-tied container and leveled as PB adsorbent, without any further treatment. The second portion of the sample was impregnated with 85% concentrated H_3PO_4 in the ratio (2:1) wt./wt and the third portion with KOH plus 100 cm^3 distilled water in the same ratio, followed by manual mixing for about 30min and was then dried separately at 110 ^oC in an electric oven

for 24hours. Using muffle furnace, the samples was carbonized at 600 ^{o}C temperature. The samples were cooled, leached with 0.1 M H_3PO_4 and 0.1 M KOH as appropriate then washed thoroughly with distilled water until a neutral (pH≈6.9) was attained. The desired activated carbon was obtained after drying in an oven at 110 ^{o}C for 24 hours.

2.4. Characterization

The adsorbents were characterized using scanning electron microscope (SEM) and Fourier transform infrared (FTIR). Ash content, moisture content, bulk density and pH of point zero charge were also determined.

2.4.1. Determination of Percentage Yield

A crucial metric for assessing an adsorbent's viability from a particular precursor is product yield (Of *et al*., 2017). The manufactured activated carbon's percentage yield (%yield) was calculated by weighing 100 g of the raw material (labeled M_b), allowing it to cool, and then recalculating its weight with an electric weighing scale as M_a. The raw material was then activated and carbonized at 600 °C.

Equation 2.1 was used to determine the precursor's percentage yield:

$$\%Yield = \frac{M_a}{M_b} \times 100 \qquad (2.1)$$

Where M_a is mass of the char and M_b is the initial mass of the sample (Adeyi *et al*., 2010).

2.4.2. Determination of Moisture Content

In order to identify the hygroscopic property of activated carbon, the moisture content was evaluated. On dry bases, the moisture content was computed. dried, spotless, empty crucible was weighted (W_1). The crucible was filled with the 2 g powdered sample of both treated and untreated biomass individually, which had been weighed (W_2). Each sample was continuously reweighed every 10 minutes after drying in an oven set at 110^{o}C, until the weight remained constant, while the crucible containing the dried powdered sample was in an oven set at 110^{o}C. The crucible and sample were weighed again (W_3). Equation 2.2 was used to calculate the moisture content from the sample's weight loss (Amran *et al*., 2011; Ohimor *et al*., 2021):

$$Moisture\ content = \frac{W_2 - W_3}{W_2 - W_1} \times 100 \qquad (2.2)$$

Where W_1 is the mass of empty crucible (g), W_2 is the mass of crucible plus sample before drying (g) and W_3 is the mass of crucible plus sample after drying (g)

2.4.3. Determination of Ash content

Crucibles were heated to around 600°C, cooled in a desiccator, and then weighed to determine the ash content. Each sample was put into the crucibles at a weight of 1.0 g before being reweighed. The samples' crucibles were then placed in the furnace, where they were heated for around 1 hour and 30 minutes to 600°C, cooled to room temperature (30°C), and then weighed again. Equation 2.3 was used to determine the ash content (Ekpete *et al*., 2017):

$$Ash\ content = \frac{ash\ weight}{Oven\ dry\ weight} \times 100 \qquad (2.3)$$

2.4.4. Determination of Bulk Density

The methods of Sugumaran *et al.* (2012) were slightly modified to measure bulk density. Powdered adsorbent sample was individually compressed to a glass cylinder (5 cm^3) to 2 cm^3 mark. Equation 2.4 was used to calculate the bulk density (g/cm^3) (Sugumaran *et al*., 2012).

$$Bulk\ desity = \frac{mass\ of\ sample\ (dry)\ (g)}{Volume\ of\ packed\ dry\ sample\ (cm^3)} \qquad (2.4)$$

All the experiments were carried out in triplicate and the averages were presented.

2.4.5. pH of point zero charge

pH of Point of Zero Charge (pH_{pzc})**:** The pH at the point of zero charge (pH_{pzc}) is a significant parameter in the study of adsorption phenomena, especially when electrostatic forces are involved. pH_{pzc} is a relevant indicator of the chemical and electronic properties of the material used as an absorbent (Ences *et al*., 2008; Benı´tez, *et al*., 2017). The salt addition method was used to measure this parameter as follows: Solutions of 50 mL of NaCl (0.1 M) were poured into a 250 cm^3 conical flask, and the initial pH (pH_i) was adjusted in each volume, ranging from 2 to 12, by adding 0.1 M solutions KOH or HCl in drops. In each flask, 0.1 g of bio-adsorbent was added. After 4 hours of agitation at room temperature, the final pH (pH_f) was measured from each solution after filtrations. On a graph with $pH_f = f(pH_i)$, the intersection of the pH curve with the bisector of the first quadrant axis resulted in the pH_{pzc} values**.** The final pH (pH_f) of each solution was assessed following filtration after 4 hours of agitation at room temperature. The pH_{pzc} value was obtained from the intersection of the pH curve with the bisector of the first quadrant axis on a graph (Ences *et al*., 2008; Benı´tez, *et al*., 2017)

2.5. Batch adsorption experiment

The experiment was carried out on an orbital incubator shaker at 200 rpm, room temperature, using 250 cm^3 conical flask which contained 100 cm^3 of the dye solution to study the effects of adsorption

conditions. The initial pH of the respective solutions were adjusted to desired values using 0.1M HCl and 0.1M KOH (Yunusa and Ibrahim, 2020). During this experiment, a certain amount of the adsorbent prepared (0.1 – 1.0 g) was added to 100 cm^3 solution of the dye. The samples were filtered after agitation and the concentration were analyzed using UV spectrophotometer. Best condition was chosen for further optimization process, by varying contact time (10-120 min), pH (2-12), concentration of dye (10-100 mg/L) adsorbent dosage (0.1-1.0 g) and temperature of 30°C-60°C. All the processes were carried out at room temperature, only for the effect of temperature where it was varied from 30-60°C.

The adsorption capacity was determined using equation 2.5

$$q_e = \frac{C_i - C_e}{M} \times V \qquad (2.5)$$

where V is the volume of the adsorbate solution, q_e is the dye uptake capacity (mg/g), M is the mass of adsorbent in g, C_i is the initial dye concentration and C_e is the dye concentration at equilibrium. The total efficiency in percent (%Removal) was calculated using equation 3.2;

$$\% R = \frac{C_i - C_e}{C_i} \times 100 \qquad (2.6)$$

2.5.1. Determination of the effect of agitation time

Method of Yunusa & Ibrahim, (2020) was used with slight modifications. The adsorbent (0.1 g) was introduced into 250 cm^3 Erlenmeyer flask containing100 cm^3 dye solution. The optimized agitation time were 10, 20, 30, 40, 60, 90, and 120 min. All other parameters including temperature (30°C), adsorbent dose (0.1 g), 200 rpm and pH (adsorbent's pH) were all kept constant.

2.5.2. Determination of the of initial concentration

The adsorbent (0.1 g) was added to 100 cm^3 of the dye of varied concentration (10, 20, 30, 50, 70 and 100 mg/L). The mixture was stirred using incubator shaker for each adsorbent's optimum time obtained, at 200 rpm and 30°C. Thereafter, the mixture was filtered and the dye concentration was measured by the absorbance obtained from UV analysis of the filtrate (Hameed and Ahmad, 2009).

2.5.3. Determination of the of adsorbent dosage

- Using the procedure reported by Yunusa & Ibrahim, (2020) with little modification, for each 100 cm^3 volume of adsorbate solution, 0.1 g of the sample was added. The studies were conducted at ambient temperature (30°C) and 200 rpm for each adsorbent's optimum time, filtered and then taken to UV analysis using UV-vis spectrophotometer, from where the concentration was detected. The optimized adsorbent dosages were 0.1, 0.3, 0.6, 0.8, and 1.0 g. The remaining adsorbents underwent the same procedure.

2.5.4. Determination of the of temperature

The method of Yunusa & Ibrahim, (2020) was slightly modified to determine the effect of temperature. Whereby a 0.1 g adsorbent was added to 100 cm^3 of adsorbent's optimum initial concentration. The mixture was agitated at respective optimum agitation time of the adsorbent, filtered and the absorbance was detected using UV-vis spectrophotometer from where the equilibrium concentration was measured from the calibration curve. The experiments were carried out at 30°C, 40°C, 50°C and 60°C. All other parameters were kept constant**.**

2.5.5. Determination of the of solution pH

The pH was tested at pH 2, 4, 6, 8, 10, and 12. For each 100 cm^3 of dye aqueous solution, 0.1 g of treated and untreated sample was added separately, after each solution had been stirred for each adsorbent's optimum time, and at the appropriate starting concentration (Hameed and Ahmad, 2009)**.** The solution was then filtered and the concentration was measured from the obtained absorbance (Yunusa & Ibrahim, 2020).

2.6. Adsorption isotherms

The importance of the adsorption isotherm in explaining how the adsorbent will interact with the adsorbate and providing a sense of adsorption capacity that cannot be overstated. They are crucial to comprehending the adsorption mechanism. The adsorption isotherm is best described using the Langmuir and Freundlich models (Yagub *et al*., 2014). It is the link between the amount of an adsorbate and the species that can absorb it (Kamaru *et al*., 2015).

2.6.1. Langmuir adsorption isotherm model

This isotherm deals with adsorbent external interactions apart from inter-individual interactions. Adsorption in a monolayer is the subject. The Langmuir model's linear form is as follows:

$$\frac{1}{q_e} = \frac{1}{q_{max}} + \left(\frac{1}{q_{max}K_L}\right)\frac{1}{C_e} \qquad (2.7)$$ (Sajid *et al*., 2022; Kamaru *et al*., 2015)

K_L is the Langmuir constant ($dm^{-3}mol^{-1}$) and q_{max} = monolayer adsorption capacity (mgg^{-1}). This equation can be simply written as:

$$\frac{C_e}{q_e} = \frac{1}{q_{max}K_L} + \left(\frac{C_e}{q_{max}}\right) \qquad (2.8)$$ (Sajid *et al*., 2022)

In general, q_{max} and K_L are functions of pH, ionic medium, and adsorbate ionic strength. When we plot a graph between Ce (mgL^{-1})/qe (mgg^{-1}) and Ce (mgL^{-1}), a straight line will be obtained. R_L, i.e., the separation factor parameter, was employed to check whether the process is favourable when $R_L > 1$ and linear for $R_L = 1$ besides irreversible for $R_L = 0$. The formula for R_L is as follows:

$$R_L = \frac{1}{1+K_L C_i} \quad (2.9)$$

where K_L = Langmuir adsorption equilibrium constant ($Lmol^{-1}$), Ci = initial dye concentration (mgL^{-1}). R_L can be determined from K_L and C_i (Sharma & Kaur 2018).

2.6.2 Freundlich Adsorption Isotherm Model

Takes into account a heterogeneous adsorption surface with unevenly distributed accessible sites and varying adsorption energies. The multilayer adsorption on the heterogeneous surface of the adsorbent is described by a non-linear empirical equation with inconsistent binding energy and unequally accessible active sites (Kamaru *et al*., 2015).

Freundlich suggested the following adsorption expression:

$$C_{ads} = K_F \mathrm{C}^{1/\mathrm{n}} \quad (2.10)$$

Integration of this equation gives the expression as:

$$\log C_{ads} = \log K_F + \frac{1}{\mathrm{n}} (\log C_e) \quad (2.11)$$

where: C_e denotes dye concentration at equilibrium ($molL^{-1}$) while C_{ads} denotes concentration adsorbed per unit mass of adsorbent ($molg^{-1}$). The Freundlich constants k_F and n represent adsorption capacity and strength, respectively. The heterogeneous adsorbent utilized is indicated by the value of n (Tariq *et al*., 2017). Adsorption happens to a greater extent when the value of n is greater than one. According to Chinniagounder *et al*. (2011) and Nasar & Shakoor (2018), n can have a value between 1 and 10 (Sajid *et al*., 2022). Good adsorption is indicated by a value of n between 2 and 10; moderate adsorption is indicated by a value of n between 1 and 2; and poor adsorption is indicated by a value of n less than 1 (Sajid *et al*., 2022). Equation 2.5 above can be resolved as follows:

$$\log q_e = K_F + \frac{1}{\mathrm{n}} \log C_e \quad (2.12)$$ (Kamaru *et al*., 2015)

where: K_F = Freundlich constant, n is the slope, q_e (mg/g) is the amount of adsorbate adsorbed per gram of an adsorbent.

There is no limit to the amount of material that can be adsorbed using this adsorption isotherm, which employs multilayer adsorption (Sajid *et al*., 2022).

2.6.3 Temkin Isotherm Model

The linear formulation of the Temkin isotherm model, which takes into account the interactions between the adsorbate and adsorbent as follows:

$$q_e = \frac{R_T}{B_T} \mathrm{In} K_T = \frac{R_T}{B_T} \mathrm{In} C_e \quad (2.13)$$

where R_T represent the universal gas constant (8.314 $Jmol^{-1}K^{-1}$) and T is the temperature of operation in kelvin. K_T (Lg^{-1}) and B_T ($kJmol^{-1}$) are Temkin isotherm constant which represent the maximum binding energy and the adsorption heat, respectively. The linear plot of q_e vs lnC_e was used to calculate the amount of K_T and B_T.

2.7. Kinetics of Adsorption

To optimize various operating parameters for the biosorption process, kinetic studies are required. The order of reaction has been explained using a variety of kinetic theories. Intraparticle diffusion, pseudo-first order, and pseudo-second order kinetic models (Fu *et al*., 2011), were used to assess the kinetics of MB dye onto biosorbents and biochars of *Parkia biglobosa* seed pod. The correlation coefficients (R^2) were measured to assess the applicability of these kinetic models (Senthamarai et al., 2012). The model may be applied to data the most effectively when R^2 is high (Yagub *et al*., 2014).

2.7.1 Pseudo-first order model

The underlying assumption of the pseudo-first order kinetic model is that the change in dye concentration with respect to time is proportional to power one. The pseudo-first order model's integral form is typically written as:

$$\log(q_e - q_T) = \log q_e - k_1 . \frac{t}{2.303} \qquad (2.14)$$ (Amran *et al*., 2011)

where k_1 is the rate constant (L min^{-1}), t is the agitation time (min), and q_e and q_t are the biosorption capacities (mgg^{-1}) at equilibrium and time t, respectively. For the biosorption of MB using biosorbents and biochars, the rate constants k_1, q_e-calculated, q_e-experimental, and R^2 values are shown in Table 4.4a and 4.4b Plotting log (q_e-q_t) versus time yields a straight line with an extremely low correlation coefficient (R^2) according to the Lagergren pseudo-first order model. (Ences *et al*., 2014)

2.7.2 Pseudo-second order kinetic model

The pseudo-second-order kinetic model explains the biosorption mechanism over the entire contact time range (Ences *et al*., 2008; Beni 'tez *et al*., 2017). The various equation is displayed below:

$$\frac{dq_t}{q_t} = k_2(q_e - q_t)^2 \qquad (2.15)$$

where K_2 (g mg^{-1} min^{-1}) is the second-order rate constant of biosorption process. By integrating and applying boundary conditions t = 0 – t and q = 0 – q_t, the above equation can be written in linear form as follows:

$$\left(\frac{t}{q_t}\right) = \frac{1}{k_2 {q_e}^2} + \frac{t}{q_e} \qquad (2.16)$$

The values of the constants k_2 (g mg^{-1} h^{-1}) and q_e (mg g^{-1}) can be determined from a plot of t/qt against

t. Table 4.4a and 4.4b displays the second order k_2, q_e-calculated, q_e-experimental, and R^2 values for the biosorption of methylene blue (MB). The results showed that the calculated and experimental q_e values are more similar. For native, processed, and immobilized biomasses, the values of the correlation coefficient (R^2) are significantly greater. Therefore, compared to pseudo-first order kinetic model, pseudo-second order kinetic model exhibits the best fit to the kinetic data and is more appropriate and efficient. These findings concur with those that were previously reported (Ences *et al*., 2014).

2.7.3 Intraparticle diffusion model

The transfer of dye molecules from an aqueous solution to the surface of a biosorbent involves a number of stages. A single step or a mixture of several steps may be used to modulate the biosorption mechanism. Film diffusion, intra-particle diffusion, or a combination of both mechanisms may be the rate-determining or rate-controlling step in the batch experiment system, which involves rapid and continuous stirring. This is how the intraparticle diffusion equation is expressed:

$$q_t = K_{diff.} t^{1/2} + C_i \qquad (2.17)$$

where K_{diff} (mg g^{-1} $min^{-1/2}$) is the rate constant of intraparticle diffusion and Ci (mg g^{-1} $min^{-1/2}$) is the intercept that characterizes the boundary layer thickness. According to the intraparticle diffusion hypothesis, the qt versus $t^{1/2}$ curve should be linear. Plotting the amount of the solid adsorbed per unit mass of biosorbent (q_t) against the square root of time ($t^{1/2}$) produced a straight line, and the particle diffusion would be the controlling step if this line passed through the origin, if the intra-particle diffusion is involved in the biosorption reaction (Bhattacharyya and Gupta 2006).

The low correlation coefficient (R^2) value suggests that intraparticle diffusion is not the main factor influencing MB biosorption onto biosorbents and biomasses. We may infer that during the biosorption of MB dye onto biosorbents and biomass, surface adsorption and intraparticle diffusion were both active.

2.8 Thermodynamic of Adsorption

To determine heat changes in a system or state of a system, some state functions, such as change in Gibbs free energy (ΔG), entropy (ΔS), and enthalpy (ΔH), were used. These parameters gave insight into the properties of the adsorption process, indicating whether it is exothermic or endothermic in nature. The following formulas can be used to calculate all of these thermodynamic properties (Vasudevan and Alothman, 2015):

$$InK_c = -\frac{\Delta H}{RT} + \frac{\Delta S}{R} \qquad (2.18)$$

Where, ΔS is the entropy, ΔH is enthalpy or total heat content of system, T is temperature, and K_c is the equilibrium constant.

$$K_C = \frac{C_{ads}}{C_e} \quad (2.19)$$

where, K_c, C_{ads} & C_e is the equilibrium constant, amount of dye adsorbed on adsorbent (mol/L) at equilibrium, and equilibrium concentration of dye left in solution (mol/L) respectively. The Gibbs free energy change will be negative if the adsorption process is exothermic. The following is the relationship between Gibbs free energy change, entropy, and enthalpy (Kamaru *et al*., 2015):

$$\Delta G = \Delta H - T\Delta S \quad (2.20)$$

3. Results and discussion

3.1. Characterization of adsorbent and adsorption test

3.1.1 Percentage Yield

Briefly, the acid-activated biomass (i.e., HPB) showed better yield of 37.33% than the base-activated carbon (i.e., KPB) which have 22.93% yield. This is due to the fact that H_3PO_4 activation enhance the conversion of aliphatic to aromatic compounds, which resulted to greater yield of char (Marie *et al*., 2019).

3.1.2 Moisture Content, Ash Content and Bulk Density

Table 3.1: Moisture Content, Ash Content and Bulk Densities of the Adsorbents

S/N	Adsorbent	Moisture Content (%)	Ash Content (%)	Bulk Density (g/cm^3)
1	PB	5	0.8	0.57
2	HPB	5.93	13	0.45
3	KPB	7.5	4.5	0.17

The higher the moisture content, the lower the adsorption capacity. Because the water (H_2O) molecule will compete with the adsorbent in trying to bind or stick to the adsorbent's active sites. Also, the higher the ash content, the lower the adsorption capacity. This is due to the fact that the mineral composition of the ash will cover or block the porous structure of the adsorbent, thereby causing depletion in dye uptake. For the bulk density, the finer the particle size, the greater the bulk density and, equally, the higher the adsorption capacity. Therefore, from the obtained results (Table 3.1), untreated biomasses (PB) will have a higher adsorption capacity due to their low moisture, ash content and greater bulk density.

3.1.3. Effect of Point of Zero Charge (pH_{pzc})

By using the solid addition method, the points of zero charge of PB, HPB and KPB were determined to be 6.6, 6.8 and 7.2 respectively, as shown in Figure 3.1. The surface charge of the biomass is negative at pH values greater than pH_{pzc}. Otherwise, the material's surface is positively charged if the pH of the

solution is lower than pH_{pzc}. At pH_{pzc}, surface charge is zero, meaning that total positive charges are equal to net negative charges (neutral surface) (Khalfaoui *et al*., 2022).

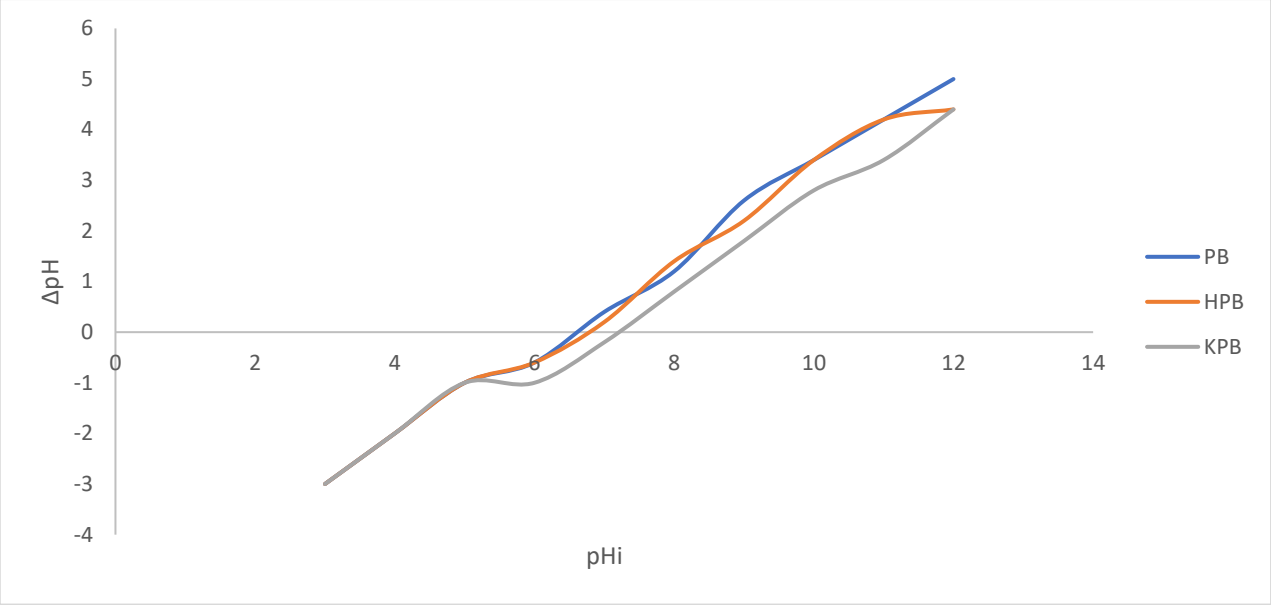

Figure 3.1: pH of point zero charge of PB, HPB and KPB adsorbent

3.1.4 Fourier Transform Infrared Spectroscopy Analysis (FTIR)

The FTIR spectra analysis of the PB samples before and after undergoing distinct treatments offers valuable insights into the alterations within the chemical composition and functional groups present on the biomass surface. In the original FTIR spectrum of the PB biomass, several prominent absorption bands were identified. A broad peak spanning the wavenumber range of 3100 to 3500 cm^{-1} indicated the presence of O-H stretching vibrations commonly associated with hydroxyl groups in alcohols and phenols (Yunusa and Ibrahim, 2020). Additionally, a double-shaped peak observed around 2900 cm^{-1} was attributed to C-H stretching vibrations in aliphatic hydrocarbons. The presence of a weak absorption band at around 2100 cm^{-1} suggested the involvement of functional groups containing triple bonds, possibly nitriles (Figure 3.2). Moreover, a sharp peak with moderate intensity at 1600 cm^{-1} was indicative of C=O stretching vibrations in carbonyl-containing groups, while a strong peak around 1000 cm^{-1} likely corresponded to ether or alcoholic C-O stretch vibrations. (Yunusa and Ibrahim, 2020), A similar result was reported by Khalfaoui *et al*. (2022). Notable transformations in the FTIR spectrum were observed after subjecting the PB biomass to acid activation and subsequent adsorption of methylene blue. The disappearance of the peaks between 3100 and 3500 cm^{-1} and around 2900 cm^{-1} indicated the removal or substantial modification of hydroxyl groups and aliphatic hydrocarbons, respectively. Interestingly, the weak band at 2100 cm^{-1} exhibited heightened intensity, signifying an increase in functional groups containing triple bonds, potentially due to the activation process (Block *et al*., 2021).

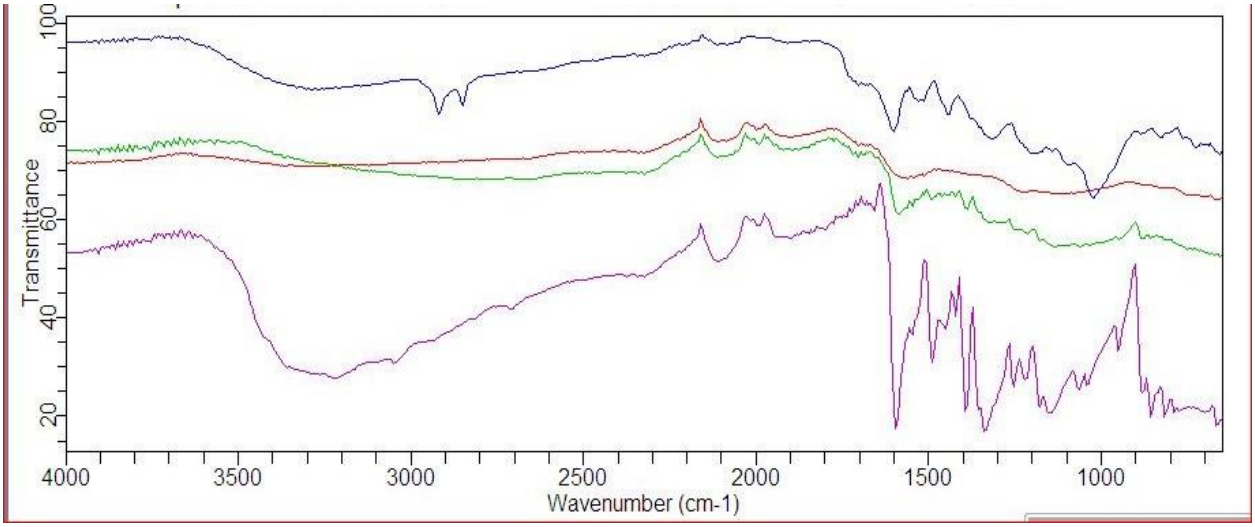

PB _____ HPB-before Adsorption_____ HPB-after Adsorption_____ MB_____

Figure 3.2: Fourier Transform Infrared spectroscopy (FTIR) Spectra of MB adsorption onto PB and HPB

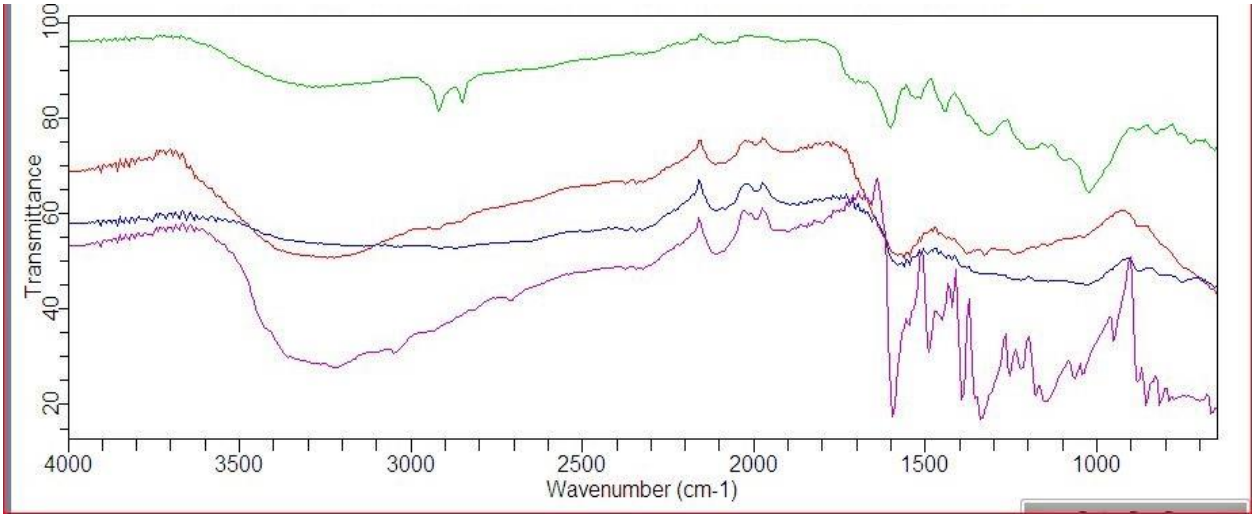

PB _____ KPB-before Adsorption_____ KPB-after Adsorption_____ MB_____

Figure 3.3: Fourier Transform Infrared spectroscopy (FTIR) Spectra of MB adsorption onto AD, HAD and KAD adsorbents

The peak at 1600 cm^{-1} remained largely unaffected by the activation treatment but displayed reduced intensity after methylene blue adsorption, suggesting interactions between the dye and carbonyl-containing groups. Furthermore, the peak at 1000 cm^{-1} vanished entirely following both activation and methylene blue adsorption, underscoring significant changes in the composition of alcohol or ether functional groups. Comparable spectral changes were observed following base activation, with a distinctive enhancement in the intensity of the broad peak between 3100 and 3500 cm^{-1}. This indicated that the base activation led to modifications similar to those induced by acid activation, albeit with a significant increase in the hydroxyl groups.

3.1.5. Surface Morphology of the Adsorbents

The morphological characteristics of the used adsorbents were assessed before and after adsorption of Methylene blue dyes and the obtained results were displayed in the following figures. The surface morphology and pore structures of PB, HPB and KPB were examined using scanning electron microscopy (SEM), and the results are shown in Figures 3.4.

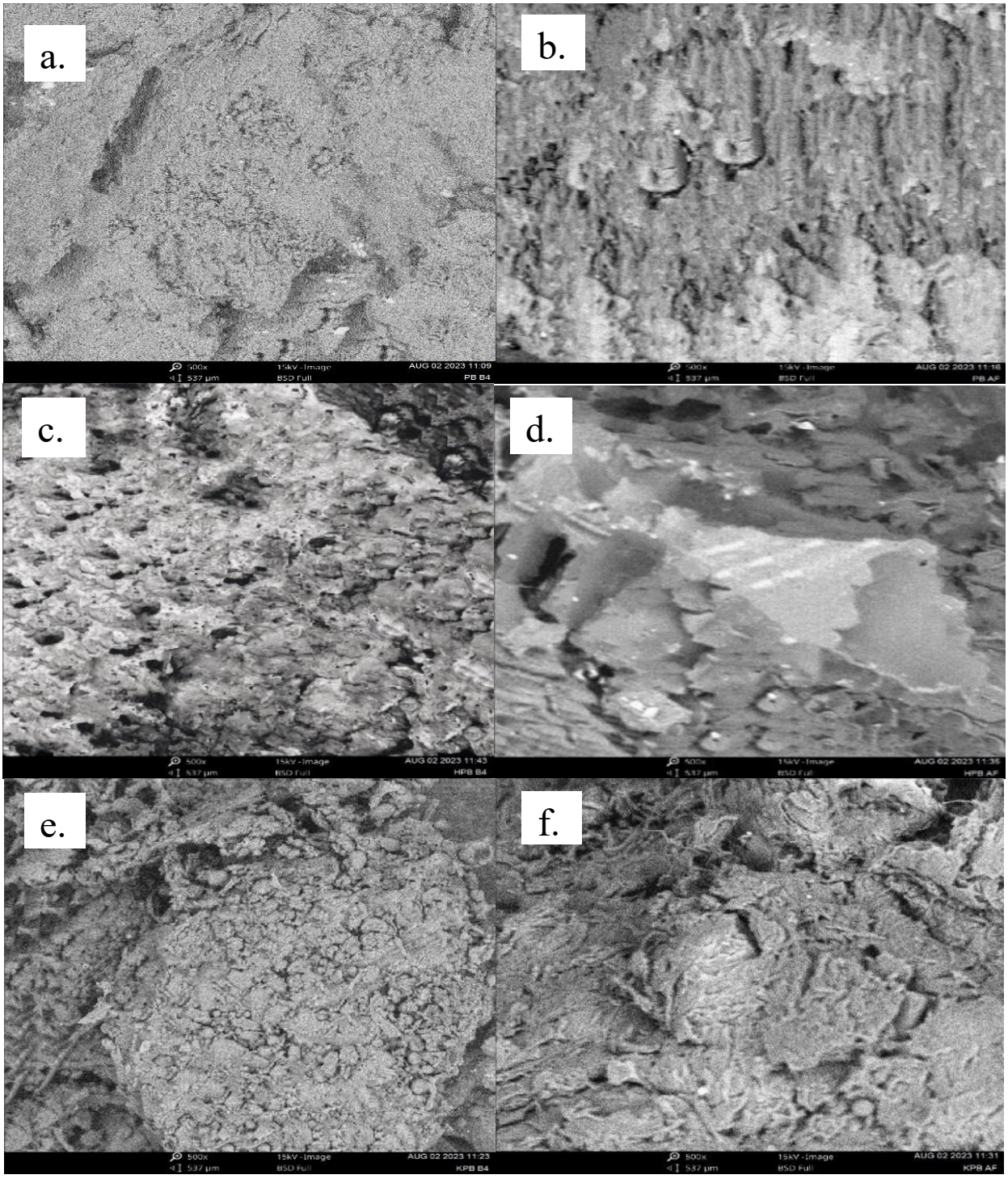

Plate 3.1: SEM micrographs (×500) of (a) PB-before, (b) PB-after, (c) HPB-before, (d) HPB-after, (e) KPB-before & (f) KPB-after adsorption

The results revealed substantial alterations in surface characteristics after pyrolysis and activation, and the SEM images of dye-loaded HPB offered insights into the dye adsorption process. SEM analysis of HPB showcased notable changes in surface morphology following pyrolysis and activation of PB using H_3PO_4 and KOH separately. The micrographs unveiled a complex network of pores and ridges, indicative of enhanced porosity and textural developments (Block *et al*., 2021). The surfaces exhibited increased roughness and irregularity compared to the original PB biomass (Zakaria *et al*., 2021and Üner *et al*., 2017). Upon adsorption of methylene blue dye, SEM images displayed the distribution of dye molecules on the PB, HPB and KPB surface. The dye molecules formed clusters on the surfaces, demonstrating effective dye adsorption. This observation suggests that the biochar's enhanced porosity, generated through the activation process, provided ample sites for dye-molecule interaction.

3.2 Effect of Operational Conditions

3.2.1. Effect of Agitation Time

A suitable adsorption system must take into account the adsorption rate. Figure 3.4 below illustrates how contact time affects the adsorption process. Figure 3.4 shows that the adsorption capacity for each adsorbate first increases quickly in the early stages, up to 19.26, 19.40 and 18.36 mg/g after reaching 40 minutes agitation time, from where the adsorption capacity started decreasing gradually with increase in agitation time, and then becomes nearly constant. Under the conditions used, further adsorption was negligible as a function of contact time after reaching equilibrium. The early, quick absorption is caused by a significant differential in concentration between the concentration of the solid surface adsorbent and the bulk liquid.

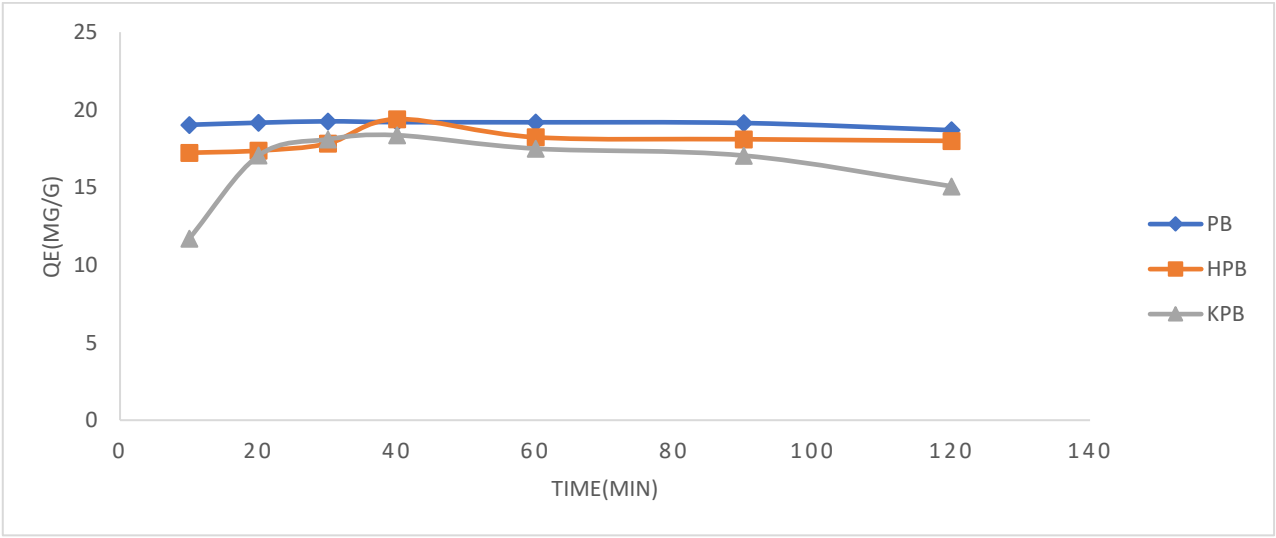

Figure 3.4: Effect of agitation time of MB adsorption onto PB, HPB, and KPB

The tiny increase in adsorption capacity at the later stages, which was mirrored by a sluggish increase, was attributed to the low number of unoccupied sites (Zubair *et al*., 2020; Ences *et al*., 2014). Adsorbate

molecules slowly fill the remaining vacant sites as a result of repulsive forces between those of the solid and liquid phases (Yunusa and Ibrahim, 2020). Therefore, 40 minutes of optimal time was chosen for further adsorption studies (Zubair *et al*., 2020). Percentage removal increases with increase in agitation time, while with further increase in contact time, desorption of dye started. This is because at saturation, dye molecules are weakly held on the adsorbent surface (Sajid *et al*., 2022). In other words, the dye molecules were impregnated into the active sites of the adsorbent at the saturation point (Sultana *et al*., 2022).

3.2.2. Effect of Initial Concentration

The initial dye concentration is known to have a significant impact on the adsorption process, which can substantially induce the solute molecules to overcome mass transfer resistance between the liquid and solid phases. Figure 3.5 illustrates how varied initial dye concentrations affect the adsorption capacity of the adsorbate, MB. It also showed the highest dye uptake of 91.48, 75.52 and 71.70 mg/g with PB, HPB and KPB respectively. An increase in adsorption capacity was observed from 9.89 to 19.76, 9.13 to 16.66, 9.44 to 18.57 mg/g onto PB, HPB and KPB with an increase in initial concentration from 10 mg/L to 20 mg/L. This may be caused by the high driving force for mass transfer at a high initial dye concentration (Kumar *et al*., 2013).

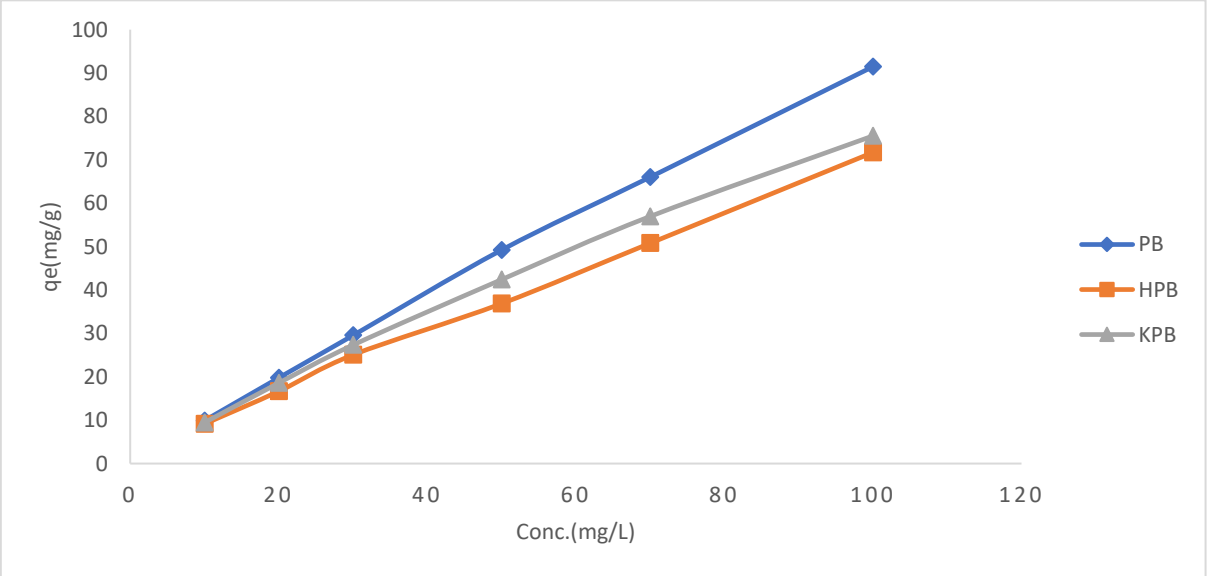

Figure 3.5: Effect of initial concentration of MB adsorption onto PB, HPB and KPB

3.2.3. Effect of Adsorbent Dosage

Figure 3.6 depicts the influence of biochar dosages of 0.1–1.0 g on the adsorption capacity of 50 mg/L concentrations of cationic MB at ambient temperature. This demonstrates the biochar's outstanding sorption capacity for the cleanup of dye-contaminated water.

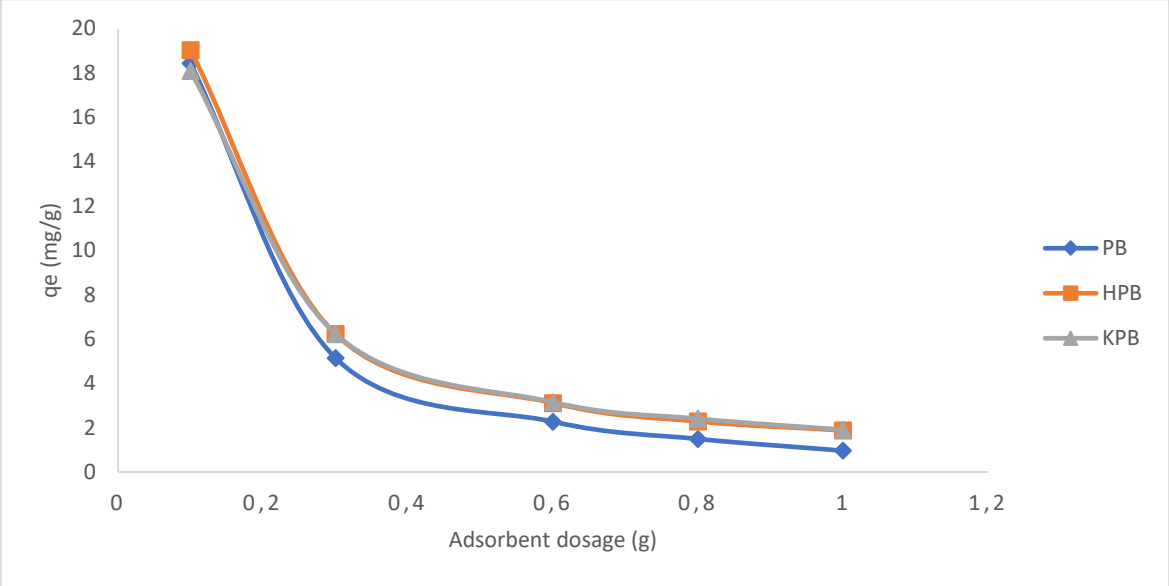

Figure 3.6: Effect of adsorbent Dosage of MB adsorption onto PB, HPB and KPB

The adsorption capacity of all three colors significantly decreased with increasing biochar dosage, as seen in Figures 3.6. But beyond a certain dose, it no longer decreased with additional biochar dosage. Using 0.1 to 0.3g of the adsorbents, the maximum adsorption capacities of the dye was determined to be 18.44 to 5.14, 1903 to 6.22 and 18.09 to 6.22 mg/g onto PB, HPB and KPB respectively. The maximum adsorption capacities of MB dye onto the aforementioned adsorbents were determined to be 18.44, 19.03 and 18.09 mg/g respectively. This demonstrates the biochar's outstanding sorption capacity for the cleanup of dye-contaminated water. Additionally, at biochar dose values above 0.4 g, a rise in dosages was followed by a decline in q_e and then became almost constant. The rise in the ratio of dye to adsorbent molecules, which leads to an improvement in dyes' sorption ability, accounts for the higher adsorption of dyes at lower biochar dosages. There may be as a result of overlap of binding sites and/or insufficient availability of dye molecules for unoccupied active sites with an increase in biochar dosage at fixed dye concentrations, resulting in reduced adsorption capability at higher dosages (Bashir, *et al*., 2021). It was observed from the results that the adsorption capacity of MB dye onto PB, HPB and KPB adsorbents, decreases with an increase in the adsorbent dosage. The decrease in the adsorption capacity was due to the attainment of equilibrium, which implies that any further addition led to desorption (Sajid *et al*., 2022).

3.2.4. Effect of Temperature

As deduced from Figure 3.7, at 303, 313, 323, and 333K, the impact of temperature on the adsorption rate of MB dye onto PB, HPB and KPB adsorbents was examined.

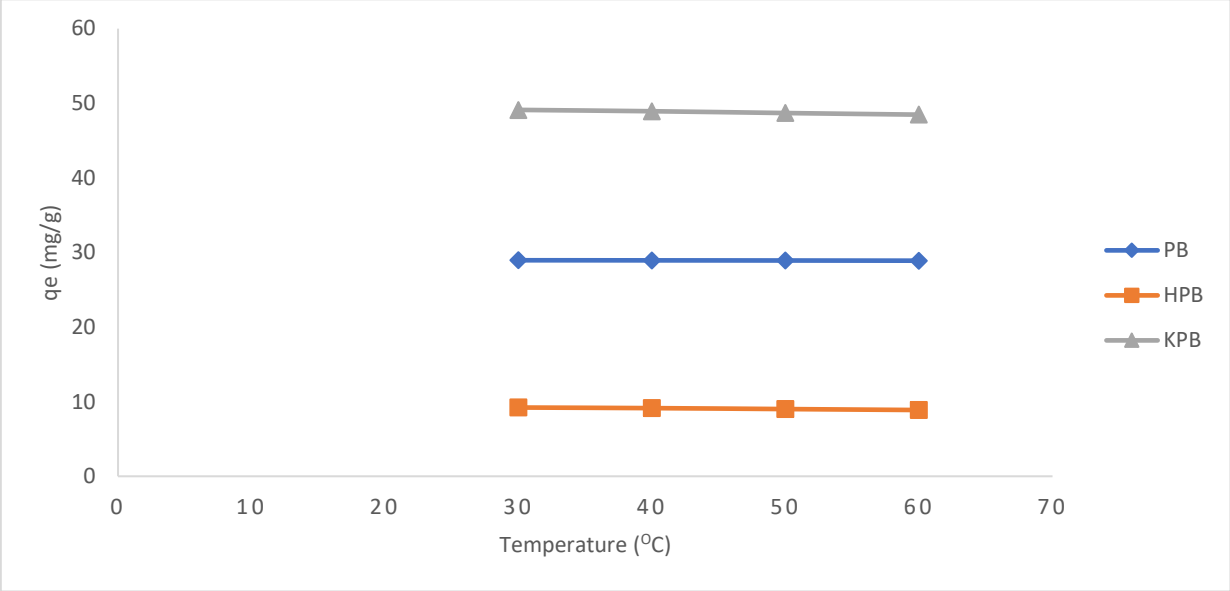

Figure 3.7: Effect of adsorbent Temperature of MB adsorption onto PB, HPB and KPB

Because of the decrease in viscosity of the solution with an increase in temperature, it is also known that raising the temperature accelerates the rate of diffusion of the adsorbate molecules past the exterior boundary layer and inside the pores of the adsorbent particle. Adsorption capacity decreased from 28.96 to 28.90, 9.22 to 8.88, and 49.12 to 48.47 mg/g onto PB, HPB and KPB adsorbents with increase in temperature (303 to 333K) that is, it is inversely proportional to temperature, implying physisorption and indicating an exothermic reaction. This might be as a result of the dye molecules being more mobile with rising temperatures. A growing number of molecules might also gather enough energy to engage with active spots (Hameed and Ahmad, 2009). The amount of dye removed is greatest at the lowest temperature, or 30^{o}C, and then it gradually decreases after that. This may be due to an increase in the kinetic energy of adsorbed molecules that are desorbed at high temperatures. Adsorbate-solvent interactions result in a decrease in the adsorption capacity as well as the percentage of dye removal because dye tends to be soluble in the solvent rather than adsorb on the adsorbent surface. Consequently, it was discovered that the process was exothermic (Sajid *et al*., 2022). Additionally, rising temperatures may have an interior swelling effect. Large dyes can penetrate more within the adsorbent's interior structure (Hameed and Ahmad, 2009).

The percentage of removal was found to decrease with an increase in temperature. This might be due to the fact that physical adsorption at higher temperatures causes a rise in entropy, which weakens the forces that bind the active sites of the adsorbent and the adsorbed species together. As a result, the fraction of adsorbed molecules may decrease due to desorption into the aqueous solution. The decrease in the adsorption capacity was due to the attainment of equilibrium, which implies that any additional increase led to desorption (Singh, *et al*., 2018).

3.2.5. Effect of pH

The overall adsorption process, and in particular the adsorption capacity, are significantly influenced by the pH of the dye solution. Figure 3.8 depicts how pH affects the used absorbents (PB, HPB and KPB) on the adsorption of MB at equilibrium.

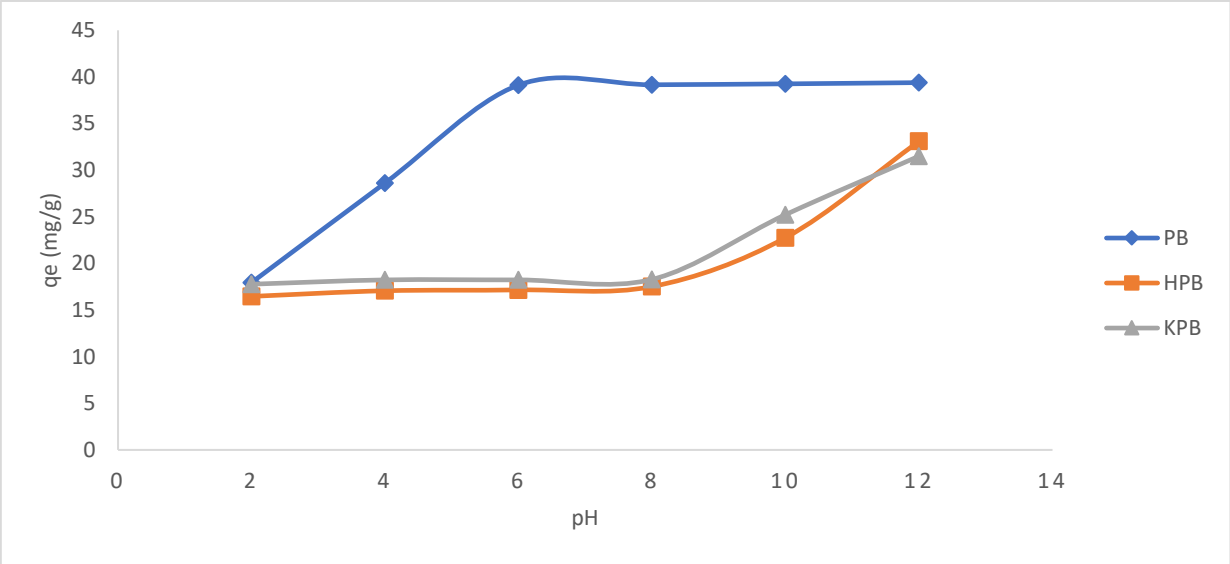

Figure 3.8: Effect of pH of MB adsorption onto PB, HPB and KPB

The q_e was discovered to rise when pH rose. The extra H^+ ions competing with the dye cations for adsorption sites were likely the cause of the lower adsorption at acidic pH (Hameed and Ahmad, 2009), whereas in basic medium, due to the excess OH^-, the surface of the adsorbent becomes negatively charged, resulting in an electrostatic attraction between the cationic dye and a negatively charged adsorbent surface, leading to improved adsorption of both the dye at basic pH (Yunusa and Ibrahim, 2020).

It is important to note in this context that the point of zero charge (pH_{zpc}), an adsorbent property, can explain the considerable impact of pH on adsorption more effectively. For both the two adsorbents, the pH_{zpc} of the biosorbents and activated carbons was discovered to be between 6.6 6.8 and 7.2 for PB, HPB and KPB respectively (Figure 3.1 and 3.2). Thus, pH_{zpc} values larger than 6.6, 6.8 and 7.2 for PB, HPB and KPB respectively, suggest that the adsorbents readily adsorb any cationic dye at pH levels higher than these values more. The fact that MB dye is cationic dye may account for the greater elimination in basic pH ranges. Therefore, the strong electrostatic interaction between the negatively charged adsorbent and the positively charged cations is the likely cause of the observed greater adsorption in basic media. Additionally, the pH of the point zero charge of the adsorbent shows that a medium with a pH higher than 6.6 is ideal for the adsorption of anionic dyes (Yunusa and Ibrahim, 2020).

3.3. Adsorption Isotherms

The relationship between a chemical's concentration in the equilibrium solution and the amount adsorbed at a constant temperature is found using adsorption isotherms. Three isotherm factors were taken into account in this study. Freundlich, Temkin, and Langmuir isotherms.

2.5.1. Langmuir Isotherm

Equations 2.7 or 2.8 provide a straight line with an intercept of $1/Kq_{max}$ and a slope of $1/q_{max}$ when plotted against C_e. The separation factor, defined in many systems using equation 2.9, is a term used to characterize the fundamental characteristics of the Langmuir isotherm. It is also referred to as the equilibrium constant (R_L).

2.5.2. Freundlich Isotherm

Plotting log q_e and log C_e using equation 2.12 results in a straight line with an intercept of (K_F) and a slope of (1/n). This is a standard method for representing experimental data to facilitate the computation of the constants (K_F) and (n) and the assessment of the success of material removal from solution.

3.3.3 Temkin Isotherm

The solution to the equation 2.13 produced a plot of q_e versus In C_e, from which the equilibrium binding constants (L/mg) corresponding to maximal binding energy could be calculated. The experimental results are given in Table 3.2. The highest R^2 values for MB dye onto PB and KPB were found to be 0.9969 and 0.9945 respectively which both correlates best with Langmuir, and Freundlich for HPB with R^2 0.9838, which are all close to unity. Therefore, MB onto PB correlates best with Langmuir > Temkin > Freundlich, MB onto HPB show best fit with Freundlich > Langmuir > Temkin and MB onto KPB have best fit Langmuir > Freundlich > Temkin Isotherm.

The separation factor parameter, R_L, for the Langmuir isotherm was used to determine whether the process is favorable or unfavorable (given in Table 4.1). The process is favorable only when $0 < R_L < 1$, while it is unfavorable when $R_L > 1$, linear for $R_L = 1$, and irreversible for $R_L = 0$ (Sajid *et al*., 2022). All the processes are favorable for Langmuir because the R_L values are less than 1 and greater than zero. Adsorption strength and capacity are represented by the Freundlich constants K_F and n, respectively. Adsorption happens more frequently when the value of n is greater than unity, n can have a value between 1 and 10 (Sajid, *et al*., 2022), the value of n represents the adsorbent's heterogeneous surface. The value of n in the range of 2–10 indicates good adsorption; a value of n between 1 and 2 indicates moderate adsorption; and a value of n less than 1 indicates poor adsorption qualities. In the current procedure, all values of n were found to be greater than unity (i.e., for MB onto both HPB and KPB the value of n is between 1 -2, indicating moderate adsorption while for MB onto PB, the n value is greater

than two, showing good adsorption), therefore obeying the condition of Freundlich isotherm (Sajid *et al*., 2022).

Table 3.2; Isotherm Parameters for Adsorption of MB dye onto PB, HPB and KPB adsorbents.

Isotherm	Parameters	PB	HPB	KPB
Langmuir	q_{max}	90.91	48.54	67.11
	K_L	1.16	0.25	0.29
	R_L	0.04	0.16	0.15
	R^2	0.9969	0.9410	0.9945
Freundlich	n	2.12	1.73	1.29
	1/n	0.47	0.58	0.78
	K_F	4.85	2.63	3.18
	R^2	0.9234	0.9838	0.9889
Temkin	B_T(J/mol)	18.09	16.64	17.10
	K_T(L/mg)	14.06	1.20	2.26
	R^2	0.9713	0.8569	0.9580

3.4. Kinetic Studies

In addition to the adsorption mechanism, the study of reaction kinetics is essential for calculating the ideal adsorption exposure time. Several kinetic models, including pseudo-first-order, pseudo-second-order, and intra-particle diffusion kinetic models, have been employed to examine the adsorption mechanism. Pseudo-first-order and pseudo-second-order models are helpful for the rate-determining stages, whereas the intra-particle diffusion model is helpful for understanding the kinetics of adsorption (Sajid *et al*., 2022). Diffusion models are typically constructed using three sequential steps: (1) solute diffusion across the liquid film surrounding the adsorbent material, or "film diffusion"; (2) solute diffusion within the adsorbent's pores, or "intra-particle diffusion"; and (3) adsorption of adsorbate on the adsorbent's active site. However, without taking into account the aforementioned phases, reaction models derived from chemical reaction kinetics are dependent on the entire adsorption process (Yunusa and Ibrahim, 2020).

The graph of t/qt against t can be used to calculate the value of the pseudo-second-order rate constant. The pseudo-first-order, pseudo-second-order and Intra-particle diffusion in (Table 3.3) models were used to fit the kinetic data acquired in this inquiry, and Table 3.3 includes the pertinent values for these models. One can infer from comparing the correlation coefficient values that the pseudo-second-order model fits the kinetic data of all the adsorbates quite well.

Table 3.3; Kinetic Parameters for Adsorption of MB dye onto PB, HPB and KPB adsorbents.

Kinetics	Parameters	PB	HPB	KPB
1st-Pseudo	q_e (mg/g)	0.05	1.32	1.20
	k_1	0.07	0.03	0.04
	R^2	0.4254	0.6044	0.5744
2nd-Pseudo	q_e (mg/g)	19.27	19.80	18.98
	k_2	0.69	0.03	0.02
	R^2	1.0000	0.9995	0.9981
Intra-particle	$q_{e.exp}$(mg/g)	19.26	19.51	18.40
	K_{diff}	0.02	0.32	0.60
	R^2	0.5171	0.7197	0.4553

Additionally, the comparison of experimental and predicted values for adsorption capacities (q_{exp} and q_{cal}) revealed that both the Intra-particle diffusion and pseudo-first-order model did not adequately explain the kinetic data, although the pseudo-second-order q_{cal} (for MB 19.27, 19.80, and 18.98 mg/g onto PB, HPB and KPB adsorbents respectively) did, by comparing with their experimental adsorption capacities (q_{exp}) of 19.26, 19.51 and 18.40 mg/g which are very close to each other (Table 3.3). Therefore, from the obtained data, pseudo-second-order model, is a better fit for representing adsorption systems. Several researchers have claimed that the pseudo-second-order model accurately captures the adsorption of metals and dyes from aqueous solutions (Yunusa and Ibrahim, 2020). The correlation coefficients of the pseudo-second order model were found to be 1.0000, 0.9995, and 0.9981 onto PB, HPB and KPB adsorbents respectively, are all close to unity, indicating the suitability of pseudo-second order model for the adsorption process.

3.5. Thermodynamic Studies

The interpretation of the nature and characteristics of the adsorption process with regard to their physicochemical features depends heavily on the thermodynamic parameters. Fundamental information regarding adsorption can be found in Gibbs free energy, adsorption enthalpy, and entropy. Gibbs free energy change (ΔG) tells us whether or not the adsorption process is spontaneous. Entropy change (ΔS) is a measure of the degree of disorder among the molecules that make up the adsorbate and the adsorbent, while enthalpy change (ΔH) provides information on the process's thermal nature, indicating whether it is exothermic or endothermic (Yunusa & Ibrahim, 2020). If ΔG is less than zero (negative), the adsorption process takes place naturally without the requirement for outside energy. ΔG > 0 (positive)

indicates that the sorption does not occur spontaneously and that the reaction mechanism needs a supportive force, usually heat energy. For the optimum adsorption process, it is typically advantageous for ΔG to be spontaneous (a negative value).

Table 3.4; Thermodynamic Parameters of MB dye adsorption onto PB, HPB and KPB adsorbents

Adsorbent	ΔH(kJ/mol)	ΔS(kJ/mol/K)	ΔG(kJ/mol)			
			30°C	40°C	50°C	60°c
PB	-1.5696	0.0225	-8.38	-8.61	-8.83	-9.06
HPB	-11.17	-0.0162	-6.25	-6.09	-5.92	-5.79
KPB	-15.65	-0.0183	-10.11	-9.93	-9.74	-9.56

From the information in table 3.4, it is clear that the entire adsorption process results in a negative ΔG, which suggests that the adsorption happens on its own without the requirement for outside energy, that is spontaneous (Imam and Babamale, 2020). It is clear that ΔH is entirely negative, indicating an exothermic process in which the adsorption capacity falls as temperature rises (Beni 'tez *et al*., 2017) . Similar behavior has also been described in another publication by; (Akter *et al*., 2021), also reported inside, that the amount of ΔH can be utilized to identify the adsorption type. Physical adsorption generates the same amount of heat as condensation, or 2.1-20.9kJmol^{-1}, but chemisorption often generates 80–200kJmol^{-1} of heat. ΔH values are within the range of 2.1-20.9kJmol^{-1}(Akter *et al*., 2021), indicating that the adsorption of MB dye onto PB, HPB and KPB are physical adsorption.

While the positive values of ΔS for the MB onto PB adsorbent indicated an increase in the randomness of the adsorbate's molecules on the solid surface of the adsorbent than in the aqueous solution, that is a positive ΔS indicates that the process follows a dissociative mechanism, also the adsorbent and adsorbate have an attraction for one another and that the degree of freedom and randomness at the solid-liquid interface are increasing (Imam & Babamale, 2020). The negative values of ΔS obtained (i.e for MB adsorption onto HPB and KPB adsorbents), suggest a decrease in the randomness of the adsorbates' molecules on the solid surface of the adsorbents than in the solution or demonstrates that unpredictability decreases near the solid-solution interface (Beni 'tez *et al*., 2017).

Conclusion

A low-cost and highly available agricultural waste, African Locust bean (Parkia biglobosa) seed pod, was found to be very effective to remove MB from synthetic wastewater. The equilibrium data were analyzed using the Langmuir, Freundlich, and Temkin isotherm models. The maximum adsorption capacities of MB were found to be 91.48, 71.70 and 75.52 mg/g onto PB, HPB and KPB respectively using 100 mg/L adsorbate concentration. Equilibrium data fitted very well with Langmuir for MB onto

PB and KPB, Freundlich for MB onto HPB adsorbent. The kinetics of the adsorption process was found to follow the pseudo-second-order kinetic model.

Conflict of Interest

The authors declare that the research was conducted in the absence of any commercial or financial relationships that could be construed as a potential conflict of interest.

References

Aaddouz M., Azzaoui K., Akartasse N., Mejdoubi E., Hammouti B., Taleb M., Sabbahi R., Alshahateet S.F. (2023). Removal of Methylene Blue from aqueous solution by adsorption onto hydroxyapatite nanoparticles, *Journal of Molecular Structure*, 1288, 135807, https://doi.org/10.1016/j.molstruc.2023.135807

Adeyi, O. (2010). Proximate Composition of Some Agricultural Wastes in Nigeria and their Potential use in Activated Carbon Production. *Journal of Applied Science Environmental Management*. 14(1) 55 - 58.

Akartasse N., Azzaoui K., Mejdoubi E., Elansari L.L., *et al.* (2022) Chitosan-hydroxyapatite bio-based composite in film form: synthesis and application in wastewater, *Polymers* 14 (20), 4265

Akter, M., Bin, F., Rahman, A., Abedin, M. Z., & Kabir, S. M. F. (2021). Adsorption Characteristics of Banana Peel in the Removal of Dyes from Textile Effluent. *Textiles*; 361–375. https://doi.org/10.3390/textiles1020018

Alshahateet S.F., Altarawneh R.M., Al-Tawarh W.M., Al-Trawneh S.A., *et al*. (2024)Catalytic green synthesis of Tin (IV) oxide nanoparticles for phenolic compounds removal and molecular docking with EGFR tyrosine kinase, *Scientific Reports* 14 (1), 6519

Aly, S. T. El-Sayed, A. M., Tharwat, K. M., Mahmoud, M.A., Khaled, A.M., Gad, A.M., Mahmoud, and A. T. (2019). Adsorption of Nile Blue Dye Using Guava Leaf Powder. *International Journal of Engineering Research and Technology (IJERT).* 8(12), 69-72.

Amran, M., Salleh, M., Khalid, D., Azlina, W., Abdul W., Idris A. (2011). Cationic and Anionic dye Adsorption by Agricultural Solid Wastes : A Comprehensive Review. *Desalination; 280*, 1–13.

Bashir, M. , Mohammed, S. Y, Atiku, M. K, Bello, A. U. , and Yakasai, H. A. (2021). Heavy Metals Content In Laboratory Wastewater : A Case Study of Selected Units of Bayero University , Kano-Nigeria. *Bayero Journal of Pure and Applied Sciences 14*(2), 174–177. http://dx.doi.org/10.4314/bajopas.v14i2.20

Belghiti M.E., Bouazama S., Echihi S., *et al.* (2020), Understanding the Adsorption of newly Benzylidene-aniline derivatives as a Corrosion Inhibitor for Carbon steel in Hydrochloric acid solution: Experimental, DFT and Molecular Dynamic Simulation Studies, *Arab. J. Chem.* 3(1), 1499-1519 https://doi.org/10.1016/j.arabjc.2017.12.003

Benıtez, S.O. J.L.B. Lozano, The municipal solid waste cycle in Mexico: Final disposal, Res, C. E. J. 150 (2009) 174–180. (2017). Kinetic Modeling of Liquid-Phase Adsorption of Congo Red Dye Using Guava Leaf-Based Activated Carbon. *Applied Water Science*, *7*(4), 1965–1977. https://doi.org/10.1007/s13201-015-0375-y

Bhattacharyya, K.G.Gupta, S.S. (2006) Adsorption of Fe(III) from Water by Natural and acid activated Clays: Studies on equilibrium Isotherm, Kinetics and Thermodynamics of Interactions. Adsorption 12,185-204 2006. https://dio.org/10.1007/s10450-006-0145-0

Biglobosa, P. (2014). *Parkia biglobosa* (African Locust Bean Tree). *World Journal of Pharmaceutical Research*. 3(2), 1672-1682

Block, I., Günter, C., Rodrigues, A. D., Paasch, S., Hesemann, P., & Taubert, A. (2021). Carbon

Adsorbents from Spent Coffee for Removal of Methylene Blue and Methyl Orange from Water.

Bouri M., Gurau M., Salghi R., Cretescu I., Zougagh M., Rios Á. (2012) Ionic liquids supported on magnetic nanoparticles as a sorbent preconcentration material for sulfonylurea herbicides prior to their determination by capillary liquid chromatography, *Analytical and Bioanalytical Chemistry*, 404, 1529-1538

Charumathi, D., and Das, N. (2012). Packed bed column studies for the removal of synthetic dyes from textile wastewater using immobilised dead C. tropicalis, *Desalination*, 285, 22–30.

Chinniagounder, T., Shanker, M. and Nageswaran, S. (2011). Adsorptive Removal of Crystal Violet Dye Using Agricultural Waste Cocoa (Theobroma cacao) Shell. R*esearch Journal of Chemical Sciences* 2231, 606X.

Dabrowski, A. (2001). Adsorption from Theory to Practice. *Advanced in Colloid and Interface Science*; 93(1-3): 135-224.

Dargo, H., Gabbiye, N., and Ayalew, A. (2014). Removal of Methylene Blue Dye from Textile Wastewater Using Activated Carbon Prepared from Rice Husk. *International Journal of Innovation and Scientific Research 9*(2), 317–325.

Garg, V.K. Gupta R. Yadav, A.B Kumar, R., Dye removal from aqueous solution by adsorption on treated sawdust, Bioresour. Technol. 89 (2003) 121–124.

Dutta, S., Gupta, B., Srivastava, S. K., & Gupta, A. K. (2021). Materials Advances Recent Advances on the Removal of Dyes from Wastewater Using Various Adsorbents : a Critical. *Royal society of Chemistry* 4497–4531. https://doi.org/10.1039/d1ma00354b

Ekpete, O. A., Marcus, A. C., and Osi, V. (2017). Preparation and Characterization of Activated Carbon Obtained from Plantain (Musa Paradisiaca) Fruit Stem. *Journal of Chemistry*. (1), 1-6.

Ences, S., Renou, J.G., Givaudan, S., Poulain, F., Dirassouyan, & Moulin, P., (2014). Landfill leachate treatment: Review and opportunity, Journal of *Hazardous Material*. 150, 468–493.

Errami M., Salghi R., Zarrouk A., Assouag M., Zarrok H., *et al*(2012), Electrochemical degradation of imazalil and pyrimethanil by anodic oxidation on boron-doped diamond, *Journal of Chemical and Pharmaceutical Research*, 4 N° 7, 3518-3525

Errami, M., Salghi, R., Zougagh, M., Zarrouk, A., Bazzi, E.H., Chakir, A., Zarrok, H., Hammouti B., Bazzi, L. (2013) Electrochemical degradation of buprofezin insecticide in aqueous solutions by anodic oxidation at boron-doped diamond electrode, *Res. Chem. Intermed.*, 39 N°2, 505-516

Fu, F., Gao, Z., Gao, L., and Li, D. (2011). Effective Adsorption of Anionic Dye , Alizarin Red S , from Aqueous Solutions on Activated Clay Modified by Iron Oxide. *Industrial and Engineering Chemistry Research*; 50(16), 9712–9717.

Haque, E., Jun, J. W., and Jhung, S. H. (2011). Adsorptive Removal of Methyl Orange and Methylene Blue from Aqueous Solution with a Metal-Organic Framework Material , Iron Terephthalate (MOF-235). *Journal of Hazardous Materials*. *185*, 507–511. https://doi.org/10.1016/j.jhazmat.2010.09.035

Hameed, B. H., & Ahmad, A. A. (2009). Batch Adsorption of Methylene Blue from Aqueous Solution by Garlic Peel , an Agricultural Waste Biomass. *Journal of Hazardous Materials*. *164*, 870–875. https://doi.org/10.1016/j.jhazmat

Imam, S. S., and Babamale, H. F. (2020). A Short Review on the Removal of Rhodamine B Dye Using Agricultural Waste-Based Adsorbents. *Asian Journal of Chemical Sciences*. *7*(1), 25–37. https://doi.org/10.9734/AJOCS/2020/v7i119013

Jaafar A, Boussaoud A, Azzaoui K, Mejdoubi *et al.* (2016), Decolorization of Basic Red 5 in aqueous solution by Advanced Oxidation Process using Fenton's reagent, *Moroccan Journal of Chemistry* 4 (3), 759-763, https://doi.org/10.48317/IMIST.PRSM/morjchem-v4i3.5206

Kamaru, A. A., Sani, N. S., Ahmad, N., and Nik, N. (2015). Raw and Surfactant-Modified Pineapple Leaf as Adsorbent for Removal of Methylene Blue and Methyl Orange from Aqueous Solution. *Desalination and Water Treatment*, 3994(11), 0–15. https://doi.org/10.1080/19443994.2015.1095122

Khalfaoui, A., Khelifi, M. N., Khelfaoui, A., Benalia, A., & Derbal, K. (2022). The Adsorptive Removal of Bengal Rose by Artichoke Leaves : Optimization by Full Factorials Design. *Water*. https://doi.org/10.3390/w14142251

Khalid, D., Amran, M., Salleh, M., Azlina, W., Abdul, W., Idris, A., and Zainal, Z. (2012). Batch Adsorption of Basic Dye Using Acid Treated Kenaf Fibre Char : Equilibrium , Kinetic and Thermodynamic Studies. *Chemical Engineering Journal*. 182, 449–457.

Kumar, K. Y., Muralidhara, H. B., Nayaka, Y. A., Balasubramanyam, J., and Hanumanthappa, H. (2013). Low-Cost Synthesis of Metal Oxide Nanoparticles ond their Application in Adsorption of Commercial Dye and Heavy Metal Ion in Aqueous Solution. *Powder Technology*, 246, 125–136.

Lamhamdi A., Azzaoui K., Mejdoubi E., Garoiz H., *et al*. (2014), Extraction of organochlorine pesticides by a matrix of calcium phosphate Moroccan Journal of Chemistry 2 (2), 90-96

Le, T. T., Murugesan, K., Lee, C-S., Vu, C. H., Chang, Y.S., and Jeon, J-R. (2016). Degradation of synthetic pollutants in real wastewater using laccase encapsulated in core–shell magnetic copper alginate beads, *Bioresource Technololy.*, 216, 203–210.

Marie A., Atia A.A., Elgogary T.M., El-Nashas A.M. (2019). Adsorption of Cu^{2+} and Mg^{2+} Ions on Silica Gel Derived from Rice Hulls ash: Experimental and Theoretical Studies. *Journal of Theoretical and Computational Chemistry*, 18(5), 1950026. https://doi.org/10.1142/S0219633619500263

Mojsov, K. Andronikov, D. Janevski, A. Kuzelov, A. and Gaber, S. (2016) "the application of enzymes for the removal of dyes from textile effluents," *Advanced technologies*. 5(1), 36-41.

Mokif, L.A. (2019). Removal Methods of Synthetic Dyes from Industrial Wastewater: A review. *Mesopotamia Environmental Journal;* 5(1), 23–40. http://dx.doi.org/10.31759/mej.2019.5.1.0040

Namane, A. Mekarzia, K. Benrachedi, N. Belhaneche-Bensemra, A. Hellal, Determination of the adsorption capacity of activated carbon made from coffee grounds by chemical activation with ZnCl2 and H3PO4, J. Hazard. Mater. B 119 (2005) 189–194.

Nasar, A. and Shakoor, S. (2018) Remediation of Dyes from Industrial Wastewater using Low-Cost Adsorbents. *Materials Research Foundations*. 15, 1–33. http://dx.doi.org/10.21741/9781945291333-1.

Pam, A. A., and Abdullah, A. H. (2022). Physicochemical Properties of Porous Activated Carbon Prepared from Palm Kernel Shell through a Low-Cost Activation Protocol. *African Journal of Science*s. *118*(9), 1–7. https://doi.org/10.17159/sajs.2022/13497 1

Of, O. (2017). Preparation of Date Seed Activation for Surfactant Recovery. *Malaysian Journal of Analytical Science.* 21(5), 1045 - 1053.

Ohimor, E. O., Temisa, D. O., and Ononiwu, P. I. (2021). Production of Activated Carbon from Carbonaceous Agricultural Waste Material : Coconut Fibres. *Nigerian Journal of Technology*. 40,(1), 19–24.

Shaban, M., Abukhadra, M. R., Aslam, A., and Khan, P. (2018). Removal of Congo Red , Methylene Blue and Cr (VI) Ions from Water Using Natural Serpentine. *Journal of the Taiwan Institute of Chemical Engineers*, 82, 102-116, https://doi.org/10.1016/j.jtice.2017.10.023

Rafatullaha, M., Sulaimana, O., Hashima, R., & Ahmadb, Anees. (2010). Adsorption of Methylene Blue on Low-Cost Adsorbents: A Review. *Journal of Hazardous Materials journal*. 177, 70–80.

Schouten, N., Van Der Ham, L. G. J., Euverink, G-J. and Haan, A. B. (2007). Selection and evaluation of adsorbents for the removal of anionic surfactants from laundry rinsing water. *Water Research*, 41, 4233 – 4241.

Singh, S., Parveen, N., and Gupta, H. (2018). Adsorptive Decontamination of Rhodamine-B from Water Using Banana Peel Powder : A Biosorbent. *Environmental Technology & Innovation*. (18), 30241-4, https://doi.org/10.1016/j.eti.2018.09.001

Sugumaran, P., Susan, V. P., Ravichandran, P., and Seshadri, S. (2012). Production and Characterization

of Activated Carbon from Banana Empty Fruit Bunch and Delonix regia Fruit Pod. *Journal of Sustainable Energy & Environment. 3*, 125–132.

Sajid, M., Javed, T., Areej, I., and Nouman, M. (2022). Sequestration of Crystal Violet Dye from Wastewater Using Low-Cost Coconut Husk as a Potential Adsorbent. *Water Science and Technology*. *85*(8), 2295–2317. https://doi.org/10.2166/wst.2022.124

Sharma, S. and Kaur, A. (2018) Various methods for removal of dyes from industrial effluents-a review. *Indian Journal of Science and Technology* 11,1–21.

Senthamarai, C., Senthil-Kumar, P., Priyadharshini, M., Vijayalakshmi, P., Vinoth-Kumar, V., Baskaralingam, P., Tiruvengadaravi, K.V., Sivanesan, S. (2012). Adsorption behavior of methylene blue dye onto surface modified Strychnos potatorum seeds. *Environ Prog Sust Energ* 32(3), 624–32.

Sultana, S., Islam, K., Hasan, M.A., Khan, H.J., Khan, M.A.R., Deb, A., Al Raihan, M., Rahman M.W. (2022). Adsorption of Crystal Violet Dye by Coconut Husk Powder: Isotherm, Kinetics and Thermodynamics Perspectives. *Environmental Nanotechnology, Monitoring & Management*, 17(9), 100651

Tariq, J., Nasir, K. and Mirza, M. L. 2017 Kinetics, Equilibrium and Thermodynamics of Cerium Removal by Adsorption on Low-Rank Coal. *Desalination and Water Treatment.* 89, 240–249.

Üner, O., Geçgel, Ü., Kolancılar, H., Bayrak, Y., Kolancılar, H., and Bayrak, Y. (2017). Adsorptive Removal of Rhodamine B with Activated Carbon Obtained from Okra Wastes. *Chemical Engineering Communications*. *6445*(4), 772-783.

Vasudevan, S., and Alothman, Z. A. (2015). Adsorption Kinetics , Isotherms , and Thermodynamic Studies for Hg Adsorption from Aqueous Medium using Alizarin Red-S-Loaded Amberlite IRA-400 Resin. *Desalination and Water Treatment*. (1) 1-9.

Yagub, M. T., Sen, T. K., Afroze, S., and Ang, H. M. (2014). Author ' s Personal Copy Dye and its Removal from Aqueous Solution by Adsorption : A Review. *Advances in Colloid and Interface Science* 209, 172–184 *Contents.* http://dx.doi.org/10.1016/j.cis.2014.04.002

Yunusa, U., and Ibrahim, M. B. (2020). Adsorptive Removal of Basic Dyes and Hexavalent Chromium from Synthetic Industrial Effluent : Adsorbent Screening , Kinetic and Thermodynamic Studies. *International Journal of Engineering and Manufacturing*. (8) 54–74. https://doi.org/10.5815/ijem.2020.04.05

Zakaria, R., Jamalluddin, N. A., and Abu Bakar, M. Z. (20121). Effect of impregnation ratio and activation temperature on the yield and adsorption performance of mangrove based activated carbon for methylene blue removal. *Results in Materials*; 10(3), 100-183. https://doi.org/10.11016/j.rinma.2021.100183

Zsilák, Z., Fónagy, O., Szabó-Bárdos, E., Horváth, O., Horváth, K., and Hajós, P. (2014). Degradation of industrial surfactants by photocatalysis combined with ozonation. *Environmental Science and Pollution Research*, 21(19), 11126 – 11134.

Zubair, M., Dalhat, N., Jarrah, N., & Blaisi, N. I. (2020). Adsorption Behavior and Mechanism of Methylene Blue , Crystal Violet , Eriochrome Black T , and Methyl Orange Dyes onto Biochar-Derived Date Palm Fronds Waste Produced at Different Pyrolysis Conditions. *Water Air Soil Pollution*. https://doi.org/10.1007/s11270-020-04595-x